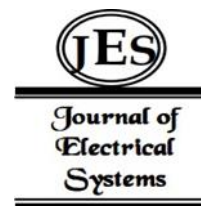


<sup>1</sup>Zikri Abadi  
Baharudin  
<sup>2</sup>Izdihartun  
Najihah Ahmad  
Daud  
<sup>2</sup>INur Asyiqin  
Mohd Isa  
<sup>2</sup>Atifa Faaidha  
Munawer

## A Statistical Analysis of Impact of Tropical Monsoon Seasons on Narrow Bipolar Pulse Characteristics



**Abstract:** - Narrow Bipolar Pulse remain a critical area of research for understanding lightning physics. With advancements in interferometry, LMA, and wavelet analysis, the ability to map and characterize these phenomena has significantly improved. However, there remains a need for deeper exploration into their interaction with physical changes property such as monsoon seasonal effect and their role in larger thunderstorm dynamics. This paper presents an improvement of the statistical information on Narrow Bipolar Pulse during Southwest Monsoon. The electric fields generated by Narrow Bipolar Pulse were recorded using High Speed Transient Recorder (Lecroy HDO4024) with 40 nanosecond resolutions in 2 seconds duration. The Narrow Bipolar Pulses (NBPs) from the South-West Monsoon season (May 2018) consist of 149 samples while 55 samples were gathered during North-East Monsoon (November 2016). In South-West Monsoon, 22 were identified as isolated NBPs, while 127 were associated with cloud-to-ground (CG) and cloud flashes. In contrast, during the North-East Monsoon, 55 NBP samples were gathered, of which 46 were classified as isolated NBPs. Furthermore, 9 samples were characterized as NBPs associated with negative CG flashes. The study found that NBPs occur much less frequently during the North-East Monsoon compared to the South-West Monsoon. This suggests that tropical monsoon seasons significantly impact the generation of Narrow Bipolar Pulses.

**Keywords:** Narrow Bipolar Pulse, Intracloud, Monsoon Seasonal

### 1. INTRODUCTION

Narrow Bipolar Pulses (NBPs) are a class of lightning signatures characterized by fast current waveforms, typically associated with a brief pulse of positive or negative polarity. These pulses have garnered significant interest due to their unique electromagnetic properties and potential to provide insights into the dynamics of lightning discharges. This review synthesizes existing research on NBPs, examining their characteristics, occurrence patterns, and advancements in their detection and analysis, especially in tropical and high-latitude regions.

Narrow Bipolar Pulses are high-intensity, short-duration electrical pulses observed during lightning events, primarily in cloud-to-ground (CG) or intracloud (IC) discharges. Their name derives from the fact that these pulses typically exhibit a narrow temporal duration and a bipolar (positive-negative) structure. NBPs are often classified into positive or negative varieties, depending on the polarity of the initial pulse in the sequence. The defining characteristics of NBPs include their steep rise time (often less than 1  $\mu$ s) and brief duration (typically in the range of 100 to 300  $\mu$ s). These pulses are usually associated with specific lightning phenomena, such as initial breakdowns or the early stages of lightning initiation, providing crucial information on the lightning channel's electrical characteristics. The propagation of these pulses is influenced by factors such as cloud height, discharge polarity, and atmospheric conditions.

The occurrence of NBPs varies across geographical regions, with some studies showing a higher frequency in tropical regions and others in mid-latitude areas. Research by [1,2] emphasized the prevalence of NBPs in tropical areas, particularly in Sri Lanka and Malaysia, where thunderstorms are frequent and intense. In contrast, studies in the United States and Europe report NBPs occurring with a lower frequency but still providing valuable data on the early stages of lightning development. The studies by [3,4] also contribute to the understanding of NBPs, particularly in regions where tropical and mid-latitude climates interact, offering insights into how latitude might influence NBP characteristics. Notably, NBPs are commonly observed during the first breakdown of lightning, as

<sup>1</sup> \*Corresponding author: Faculty of Electrical Engineering Technology Engineering, Universiti Teknikal Malaysia Melaka

<sup>2</sup> Author: Faculty of Electrical Engineering Technology Engineering, Universiti Teknikal Malaysia Melaka

\*Corresponding author email: zikri@utem.edu.my

Copyright © JES 2024 on-line : journal.esrgroups.org

seen in the research by Karunarathne and co-workers [3], which identified the relationship between NBPs and lightning initiation.

One significant advancement in NBP research is the development of high-resolution mapping technologies, including Lightning Mapping Arrays (LMA) and interferometry-based techniques. The use of LMA, as outlined by Zakaria and co-workers [5] and Gunasekara and co-workers [6], has allowed for the precise localization of NBPs within the lightning channel. These systems work by detecting and mapping the high-frequency electromagnetic emissions produced during lightning discharges. This high-resolution capability is crucial for understanding the spatial dynamics of NBPs and their relationship with the overall lightning discharge structure. Interferometry has also been employed to study NBPs in greater detail. As shown in the work of [4,7,8], using interferometric methods allow for accurate measurements of the electric field changes associated with NBPs, offering insights into their duration, intensity, and propagation characteristics. By combining these techniques, researchers can construct detailed models of NBP behavior, improving our understanding of the lightning initiation process. Moreover, the application of mapping arrays and source localization techniques has facilitated the tracking of NBP events in real-time, which was not possible with earlier measurement methods. Studies by [3,4,7,8] demonstrated the effectiveness of these tools in detecting the subtle electromagnetic signatures associated with NBPs, leading to a deeper understanding of their role in the lightning process.

Theoretical and computational advancements have also contributed to the field, with several studies proposing new models to explain the origin and propagation of NBPs. For example, [9] developed a current propagation model to simulate the behavior of NBPs within the lightning channel. This model provided a better understanding of the electrical dynamics underlying NBPs, including their formation, propagation speed, and the role of the surrounding atmosphere. In addition, [10] proposed a new current waveform model that allows for a more accurate representation of the time and current profiles associated with NBPs. These models have significantly improved the accuracy of NBP predictions and their incorporation into broader lightning discharge simulations.

NBPs have several important applications in the study of lightning physics and weather phenomena. By analyzing the characteristics and occurrence of NBPs, scientists can infer key information about lightning initiation processes, such as the conditions necessary for the formation of lightning leaders and the role of electron avalanches in lightning discharges. Research by [11-18] has demonstrated the importance of understanding the electric field changes associated with NBPs for improving lightning prediction and safety measures. Furthermore, the study of NBPs provides valuable insights into the underlying mechanisms of lightning radiation, particularly in terms of the high-frequency components that are often observed during the initiation of lightning flashes. Studies by [19,20] have emphasized the role of NBPs in the electromagnetic radiation spectrum, offering new perspectives on the potential applications of NBP analysis in lightning detection and warning systems.

This study examines the NBP under the influence of Southwest monsoon and Northeast monsoon season. We examine the profile of the NBP using atmospheric electricity sign convention where the feature of positive charges moving down to the earth direction (or negative charges transported upward) produces an electric field change as shown in Figure 1. This NBP signature is known as positive NBP (+NBP). The negative charges moving down (or positive charges transported upward) produces an electric field change. This NBP signature is known as negative NBP (-NBP). This study has found two types of narrow bipolar pulse (NBP): isolated pulse of NBP and the NBP associated with ground flash. This study also presenting the results of Rising Time 0-100%, Rising Time 10-90%, Peak Amplitude (V), Duration NBP Pulse ( $\mu\text{s}$ ), Zero Crossing Time (ZCT ( $\mu\text{s}$ )), Overshoot (V), Ratio (Os/A) and FullWidth Half Maximum (FWHM ( $\mu\text{s}$ )). Finally, the finding of isolated NBP and NBP associated with ground flash or cloud flashes were compared.

## 2. METHODOLOGY

The electric field measuring sensors are similar with the measurement layout performed by [21-27]. The operations of the antennas for electric field radiation (fast field) comprehensively was described in [22] (see Figure 2 and 3). The measurements of the electric field generated by the lightning flashes was conducted in PayaRumput, Malaysia. The electric field measurements of the whole flashes were recorded in one station in May 26, 2018, during the rainstorm monsoon period in the southern part of Peninsular Malaysia near equator and also in November 11, 2016 during the rainstorm monsoon period in the northern part of Peninsular Malaysia. The single station in Paya Rumput were located at the latitude of  $2^{\circ}18'07, 6''\text{N}$ , and the longitude of  $102^{\circ}12'13.4''\text{E}$ , respectively.

One parallel flat plate antenna was used to detect the broadband radiation electric field (or fast field). The flat antenna was used to sense the vertical electric field. In the interest of avoiding the horizontal component of electric field, the plane of the antenna is adjusted perpendicular to the electric field vector or in other words, parallel to the ground. The physical height of the antenna is 1.5 m and the effective height is 0.25 m. The antenna was connected to the electronic buffer circuit by using 60 cm long coaxial cable (RG58). Using the 10 m long coaxial cable (RG-58), the signal from the antenna is transmitted into 12-bit digital transient recorder (Lecroy HDO4024) equipped with 200 MHz High- Definition Oscilloscope. The sampling rate was set to 25 MS/s and the total duration of waveform recorded being 2 s. The trigger setting of the oscilloscope was such that signals of both polarities could be captured. The trigger level is set either 50 mV to 500 mV for the far flashes or 500 mV to 2 V for the close flashes. The transient recorder was operated at a 300 ms pre-trigger mode. The rise time of the broadband antenna system (fast field) for step input pulses was less than 30 ns, while the decaying time constant was set to approximately 15 ms. Any ambiguity of the whole flashes event such as two flashes event for the ground flashes and unclear profile of preliminary breakdown pulse were discarded in the analysis.

### 3. RESULTS AND DISCUSSION

#### 3.1 South-West Monsoon Narrow Bipolar Pulse

During May 2018, which falls within the South-West Monsoon season, a sample of data was collected. A total of 262 samples were obtained, out of which 149 were identified as Narrow Bipolar Pulses (NBPs). Among these, 22 samples were isolated NBPs, while 127 were associated with cloud-to-ground and cloud flashes. The analysis and summary of the results are detailed in the following sections.

##### 3.1.1 Isolated Narrow Bipolar Pulse During South-West Monsoon

Table 3.1 summarizes the profile of isolated narrow bipolar pulses. Out of the 262 samples, 22 were characterized as isolated NBPs, with 20 being positive and 2 negative. There was no significant difference in parameters between positive and negative NBPs, so all parameters were combined for summary. The duration of NBPs ranged from 6.63  $\mu$ s to 76.88  $\mu$ s, with an arithmetic mean of  $28.37 \pm 19.15$   $\mu$ s and a geometric mean of 23.1  $\mu$ s. The zero-crossing time (ZCT) ranged from 2.65  $\mu$ s to 10.14  $\mu$ s, with an arithmetic mean of  $5.10 \pm 1.74$   $\mu$ s and a geometric mean of 4.84  $\mu$ s.

The rise time (10-90%) had a minimum value of 0.29  $\mu$ s and a maximum of 2.87  $\mu$ s, with an arithmetic mean of  $1.33 \pm 0.7$   $\mu$ s and a geometric mean of 1.14  $\mu$ s. The full width at half maximum (FWHM) ranged from 0.92  $\mu$ s to 2.60  $\mu$ s, with an arithmetic mean of  $1.78 \pm 0.45$   $\mu$ s and a geometric mean of 1.73  $\mu$ s. Table 3.1 also shows the ratio between the peak amplitude (Pa) and the overshoot (Os), with a minimum ratio of 1 and a maximum of 13.23, an arithmetic mean of  $4.72 \pm 2.54$ , and a geometric mean of 4.20. For qualitative analysis, histograms for NBP duration, ZCT, rise time, and FWHM were created, as shown in Figure 3.1.

Figure 3.1(a) presents the histogram for the duration of isolated NBPs, showing a left-skewed pattern with most durations between 10 to 20  $\mu$ s. The standard deviation is about 67.5% of the mean, likely due to five samples exceeding 40  $\mu$ s. Figure 3.1(b) shows the histogram for ZCT duration, with the highest frequency between 2  $\mu$ s to 4  $\mu$ s. The rise time (10-90%) commonly falls between 1.8 to 2.4  $\mu$ s, as depicted in (see Figure 3.1 (c)). Understanding the energy profile of Narrow Bipolar Pulses (NBP) is crucial. Figure 3.1(d) illustrates the average duration of energy contribution for NBP. Our findings indicate that the highest frequency duration of Full Width at Half Maximum (FWHM) for isolated NBP ranges between 1.75 to 2 ms.

**Table 3.1: Statistical result of Isolated Narrow Bipolar Pulse (Pa: Peak Amplitude; Os:Overshoot)**

Features	NBP Duration (μs)	ZCT (μs)	Time Rise (μs)0-100%	Rising Time (μs)10%-90%	FWHM (μs)	Ratio Pa/Os
no of sample	22	22	22	22	22	22
min	6.32	2.65	0.83	0.29	0.92	1
max	76.88	10.14	5.17	2.87	2.6	13.23
Arith. mean	28.37	5.10	2.46	1.33	1.78	4.72
Geo. mean	23.10	4.84	2.18	1.14	1.73	4.20
median	20.88	4.94	2.05	1.22	1.85	3.99
Std. dev	19.15	1.74	1.23	0.7	0.45	2.54

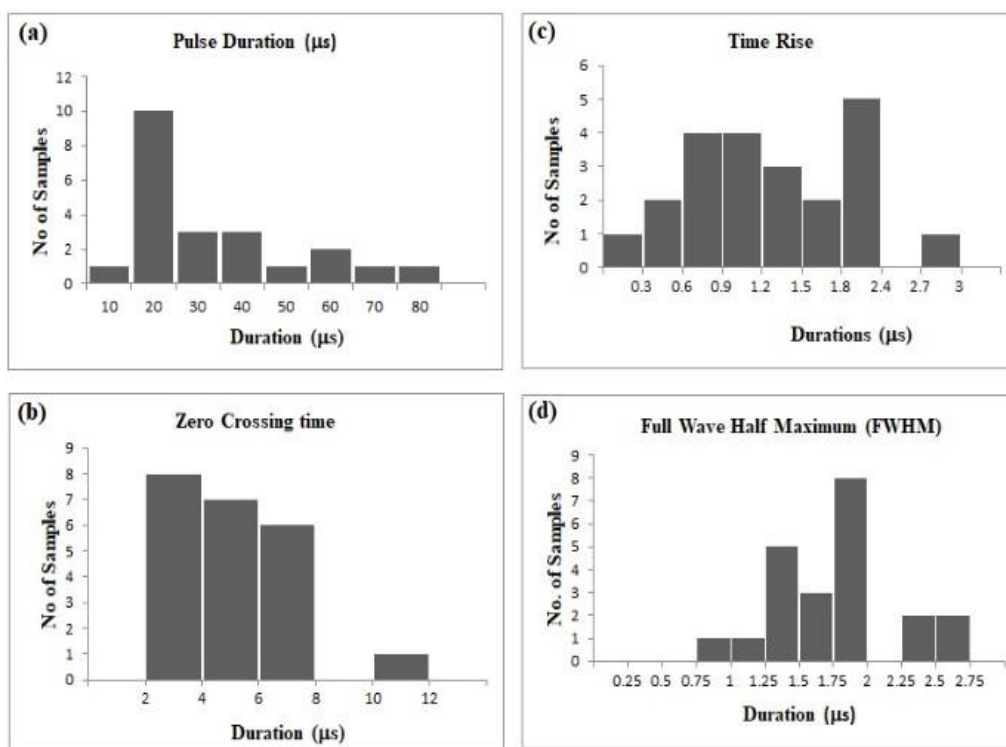


**Figure 3.1: (a) Isolated Narrow Bipolar Pulse Duration; (b) Zero Crossing Time of Isolated NBP; (c) Time Rise (10-90%) of isolated NBP; (d) Full Wave Half Maximum (FWHM)**

### 3.2 Narrow Bipolar Pulse Associated with Negative Ground Flashes and Cloud Flashes (South-West Monsoon)

Many researchers have reported that NBP features typically occur before the initial breakdown process (preliminary breakdown pulse) of negative ground flashes. Interestingly, Ahmad M.R. and his co-authors were the first to report the existence of NBP after the first return stroke of negative ground flashes or between stroke intervals. However, there is no statistical analysis supporting their data. Figures 3.2 and 3.3 provide examples of NBP features associated with negative ground flashes before the initial breakdown and after the first return stroke, respectively.

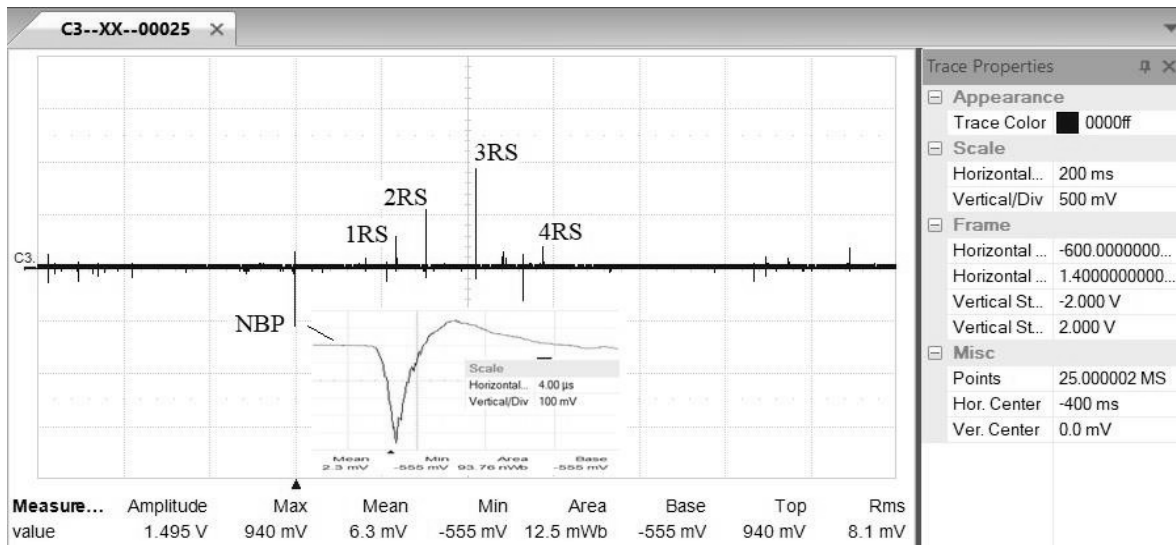


**Figure 3.2: NBP associated with negative ground flash. NBP appear before the initial breakdown or return stroke (RS-Return Stroke). This figure also provides close up picture of NBP with the scale of 4.00 ms/div and 100 mV/div.**

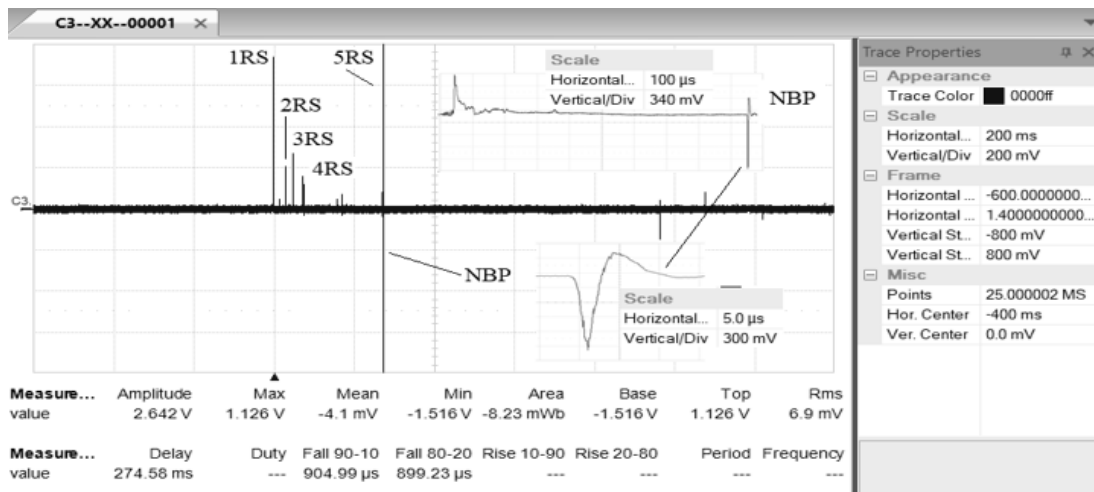


**Figure 3.3: NBP associated with negative ground flash. NBP appear after the first return stroke (RS-Return Stroke). This figure also provides close up picture of NBP with the scale of 5 ms/div and 300 mV/div.**

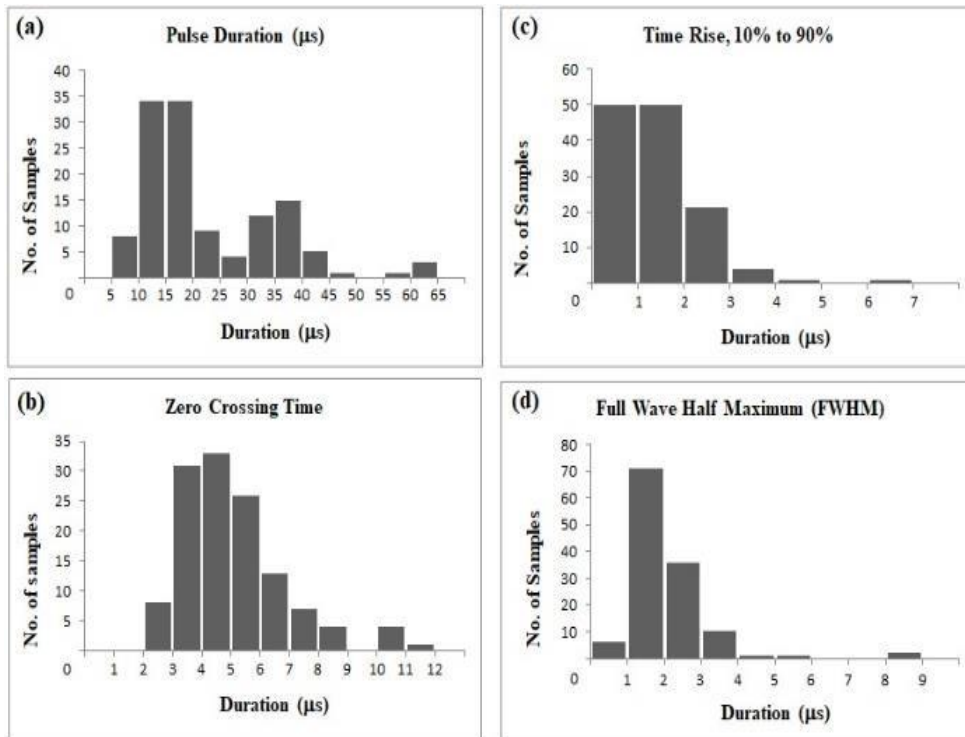


**Figure 3.4: (a) Narrow Bipolar Pulse associated with negative cloud-to-ground flash and associated with the cloud flashes. (a) Pulse Duration; (b) Zero Crossing Time of NBP; (c) Time Rise (10-90%) of NBP; (d) Full Wave Half Maximum (FWHM) of NBP**

Table 3.2 summarizes 127 out of a total of 262 samples characterized as Narrow Bipolar Pulses (NBP) associated with negative ground flashes and cloud flashes, with sample numbers of 90 and 37, respectively. Of the 90 samples, 75 appeared before the Preliminary Breakdown Pulse (PBP) and 15 after. In this analysis, we found that the number of negative NBP samples is very low and insignificant to separate from positive NBP samples. Therefore, we included both polarities of NBP as a single data group.

The duration of NBP ranged from 6.88 µs to 66.4 µs, with an arithmetic mean of  $23.03 \pm 13.08$  µs and a geometric mean of 20.0 µs. The Zero Crossing Time (ZCT) ranged from 2.16 to 11.21 µs, with an arithmetic mean of  $5.11 \pm 1.8$  µs and a geometric mean of 4.84 µs. The rise time (10–90%) had a minimum value of 0.3 µs and a maximum of 6.67 µs, with an arithmetic mean of  $1.42 \pm 0.93$  µs and a geometric mean of 1.17 µs. The Full Width at Half Maximum (FWHM) ranged from 0.53 µs to 8.82 µs, with an arithmetic mean of  $2.04 \pm 1.12$  µs and a geometric mean of 1.73 µs. The ratio (Pa/Os) had a minimum value of 2.15 and a maximum of 30.19, with an arithmetic mean of  $5.88 \pm 5.16$  and a geometric mean of 4.67.

Figure 3.4(a) shows the histogram for the duration of NBP associated with negative cloud-to-ground flashes and cloud flashes. The majority of duration pulses lie between 10 to 20 µs, similar to the case of isolated NBP. The standard deviation is about 56.8%. According to the histogram in Figure 3.4(b), the maximum frequency of NBP associated with ground flashes and cloud flashes for ZCT is between 4 µs to 5 µs, which is almost twice that of the isolated NBP case. The rise time (10–90%) lies between 0 to 2 µs (see Figure 3.1(C)). The highest frequency duration of FWHM for isolated NBP appeared between 1 to 2 µs, showing a similar trend compared to the isolated case. Overall, the results of isolated NBP are almost similar to the mixed profile of NBP, as depicted in Table 3.2.

**Table 3.2: NBP associated with the negative cloud-to-ground flash and cloud flashes**

Features	NBP Duration ( $\mu$ s)	ZCT ( $\mu$ s)	Time Rise ( $\mu$ s)0-100%	Rising Time ( $\mu$ s) 10%-90%	FWHM ( $\mu$ s)	Ratio Pa/Os
no of sample	127	127	127	127	127	127
min	6.88	2.16	0.61	0.3	0.53	2.15
max	66.4	11.21	7.97	6.67	8.82	30.19
Arith. mean	23.03	5.11	2.45	1.42	2.04	5.88
Geo. mean	20.00	4.84	2.13	1.17	1.85	4.67
median	16.92	4.76	2.14	1.17	1.82	3.81
Std. dev	13.08	1.80	1.31	0.93	1.12	5.16

Next, the results in Table 3.2 were separated into two categories: NBPs associated with negative cloud-to-ground flashes that appear before the preliminary breakdown pulse (as depicted in Table 3.3) and NBPs associated with negative cloud-to-ground flashes that appear after the first return stroke (as depicted in Table 3.4). Furthermore, by considering the arithmetic mean and geometric mean values for all parameters, we found that the values in Table 3.3 and Table 3.4 were similar to each other.

**Table 3.3: NBP associated with the negative cloud-to-ground flash appear before the preliminary breakdown pulse**

Features	NBP Duration ( $\mu$ s)	ZCT ( $\mu$ s)	Time Rise ( $\mu$ s)0-100%	Rising Time ( $\mu$ s) 10%-90%	FWHM ( $\mu$ s)	RatioPa/Os
No. of sample	75	75	75	75	75	75
Min	7.23	2.16	0.69	0.31	2.15	0.68
max	61.06	11.21	5.94	4.56	24.71	8.82
Arith. mean	23.88	5.15	2.42	1.42	5.56	2.11
Geo. mean	20.86	4.85	2.13	1.18	4.58	1.87
Median	18.24	4.69	2.14	1.17	3.94	1.81
Std. dev	12.90	1.91	1.22	0.87	4.46	1.33

On one hand, when comparing the parameters of NBP duration, ZCT, and Time Rise between the results in Tables 3.3 and 3.4 with those in Tables 3.1 and 3.2, similar results are observed. On the other hand, the FWHM in Table 3.3 differs from the result in Table 3.1 by factors of 3.12 and 2.64, respectively.

**Table 3.4: NBP associated with the negative cloud-to-ground flash appear after the first return stroke**

Features	NBP Duration ( $\mu$ s)	ZCT ( $\mu$ s)	Time Rise ( $\mu$ s)0-100%	Rising Time ( $\mu$ s) 10%-90%	FWHM ( $\mu$ s)	Ratio Pa/Os
no of sample	15	15	15	15	15	15
Min	9.62	2.98	0.7	0.3	2.40	0.96
Max	33.17	7.74	4.77	2.97	17.92	3.78
Arith. mean	19.01	4.32	2.15	1.27	5.78	1.82
Geo. mean	17.84	4.17	1.93	1.10	4.57	1.73
median	15.84	3.99	2.07	1.14	3.70	1.73
Std. dev	7.16	1.27	1.03	0.69	5.06	0.65

Furthermore, the FWHM in Table 3.3 is almost double compared to the result in Table 3.2, with arithmetic and geometric means differing by factors of 3.24 and 3.4, respectively. Additionally, similar differences in FWHM were found when comparing Table 3.4 with Tables 3.1 and 3.2. We also observed differences in the Ratio Pa/Os when using the same comparative analysis procedure as for FWHM. Therefore, based on this analysis, it is important to separate the data of isolated NBPs from NBPs associated with cloud flashes, as the parameters of FWHM and the ratio of Pa/Os show significant differences compared to NBPs associated with negative ground flashes. Anyone planning to analyze the sub-microsecond structure of pulses must distinguish between isolated cases and NBPs associated with flashes (ground or cloud flashes). Our results are consistent with [13,14,17], where NBPs typically occur uniquely as isolated pulses or prior to the PBP of ground flashes. Interestingly, NBPs can also appear following the return stroke, consistent with the report by [17]. We performed significant statistical analysis on NBPs following the return stroke. Next, the North-East Monsoon data of NBPs will be presented in the upcoming subtopic.

### 3.3 North-East Monsoon Narrow Bipolar Pulse

A set of data under the North-East Tropical Monsoon was obtained in November 2016. Similar to the South-West Tropical Monsoon, the data was analyzed by considering several parameters as mentioned before. Histograms are presented to show and compare the significant differences or similarities between isolated NBPs and NBPs associated with ground flashes. As with the South-West Tropical Monsoon analysis, NBPs associated with ground flashes are classified into two categories: NBPs occurring before ground flashes and NBPs occurring after ground flashes. The details of the analysis and summary of the results are presented in the following subtopics.

### 3.4 Isolated Narrow Bipolar Pulse (North-East Monsoon)

The isolated narrow bipolar pulse profile is summarized in Table 3.5. Out of a total of 312 samples, 46 are characterized as isolated NBPs, with 9 positives isolated NBPs and 37 negative NBPs. The duration of NBPs ranges from 11.48  $\mu$ s to 40.95  $\mu$ s, with arithmetic and geometric means of  $23.77 \pm 6.81$   $\mu$ s and 22.75  $\mu$ s, respectively. The ZCT ranges from 2.91  $\mu$ s to 6.32  $\mu$ s, with arithmetic and geometric means of  $4.84 \pm 0.75$   $\mu$ s and 4.77  $\mu$ s, respectively. The rise time (10-90%) ranges from 0.354  $\mu$ s to 1.21  $\mu$ s, with arithmetic and geometric means of  $0.68 \pm 0.17$   $\mu$ s and 0.66  $\mu$ s, respectively. The FWHM ranges from 0.69  $\mu$ s to 3.39  $\mu$ s, with arithmetic and geometric means of  $2.04 \pm 0.48$   $\mu$ s and 1.98  $\mu$ s, respectively. Table 3.5 also shows the profile of the ratio between the peak amplitude (Pa) and the overshoot (Os). The minimum and maximum ratios (Pa/Os) are -0.64 and -0.08, respectively, with an arithmetic mean of  $-0.28 \pm 0.08$ . The histogram for NBP duration, ZCT, rise time, and FWHM is depicted in Figure 3.5.

**Table 3.5: Statistical result of Isolated Narrow Bipolar Pulse during North-East Monsoon (Pa: Peak Amplitude; Os: Overshoot)**

Features	NBP Duration ( $\mu$ s)	ZCT ( $\mu$ s)	Time Rise ( $\mu$ s)0-100%	Rising Time ( $\mu$ s) 10%-90%	FWHM ( $\mu$ s)	Ratio Pa/Os
no of sample	46	46	46	46	46	46
min	11.48	2.91	0.94	0.35	0.69	-0.64
max	40.95	6.32	4.56	1.21	3.39	-0.08
Arith. mean	23.77	4.84	1.76	0.68	2.04	-0.28
Geo. mean	22.75	4.77	1.68	0.66	1.98	-
median	24.88	4.91	1.63	0.67	1.99	-0.28
Std. dev	6.81	0.75	0.62	0.17	0.48	0.08

Figure 3.5(a) shows the histogram for the duration of NBPs in the case of isolated pulses. This figure indicates a left-skewed pattern, with the majority of isolated narrow bipolar pulse (NBP) durations falling between 12 to 16  $\mu$ s. The standard deviation is approximately 28.65% of the mean. In the histogram shown in Figure 3.5(b), the

maximum frequency of isolated NBPs for zero crossing time (ZCT) duration is between 3  $\mu\text{s}$  to 5  $\mu\text{s}$ . Typically, the highest rise time (10–90%) is between 0.5 to 1  $\mu\text{s}$ , as seen in Figure 3.5(c). Understanding the energy profile of NBPs is important; therefore, Figure 3.5(d) shows the average duration of energy contribution for NBPs. We found that the highest frequency duration of FWHM for isolated NBPs appeared between 1.5 to 2  $\mu\text{s}$ .

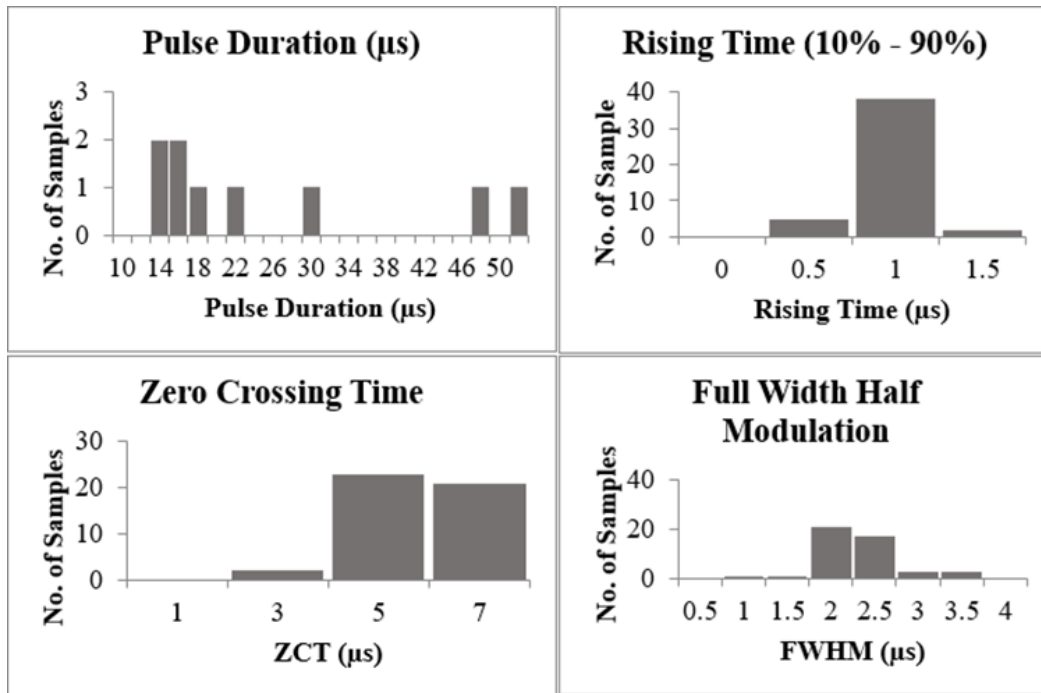


Figure 3.5: (a) Isolated Narrow Bipolar Pulse Duration; (b) Zero Crossing Time of Isolated NBP; (c) Time Rise (10-90%) of isolated NBP; (d) Full Wave Half Maximum (FWHM)

### 3.5 Narrow Bipolar Pulse associated with the negative ground flash and cloud flashes (North-East Monsoon)

Figure 3.6 and 3.7, show the examples of the features NBP associated with the negative ground flash before the initial breakdown and after the first return stroke, respectively.

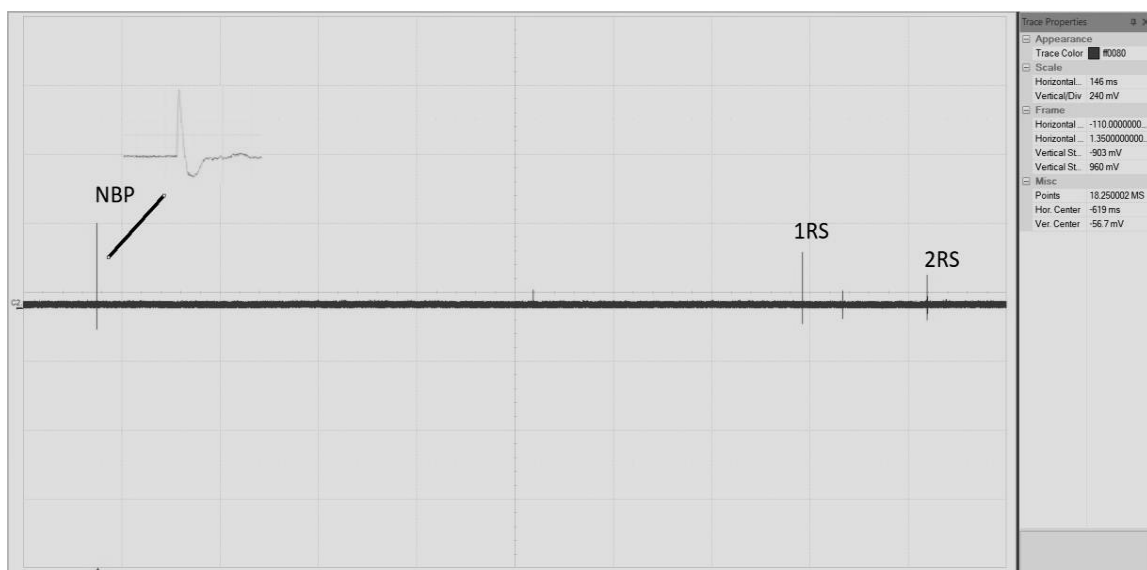


Figure 3.6: NBP associated with negative ground flash. NBP appear before the initial breakdown or return stroke (RS-Return Stroke). This figure also provides close up picture of NBP.

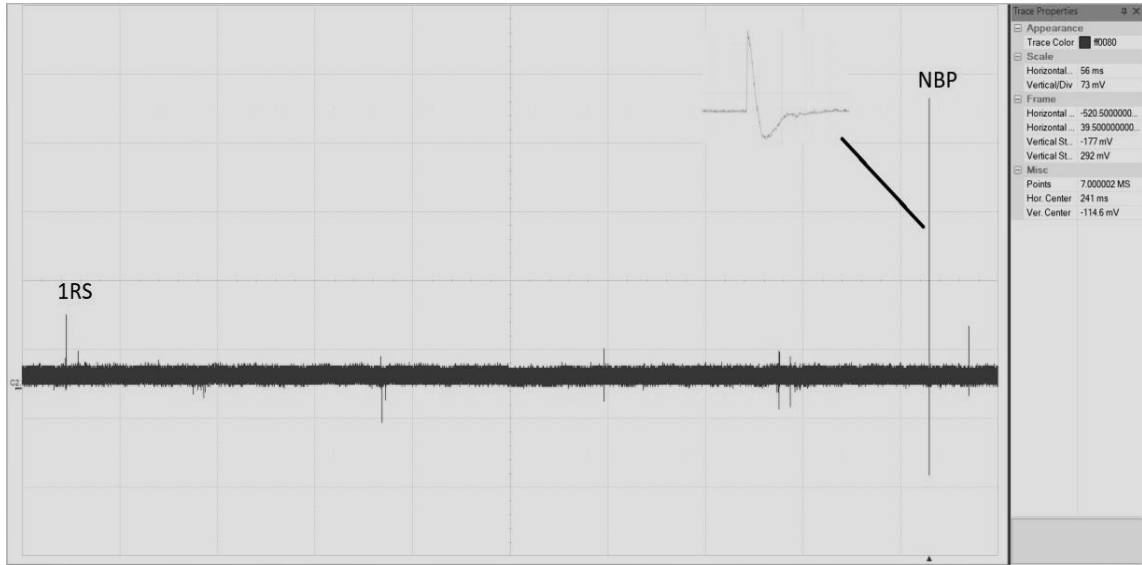


Figure 3.7: NBP associated with negative ground flash. NBP appear after the first return stroke (RS- Return Stroke). This figure also provides close up picture of NBP.

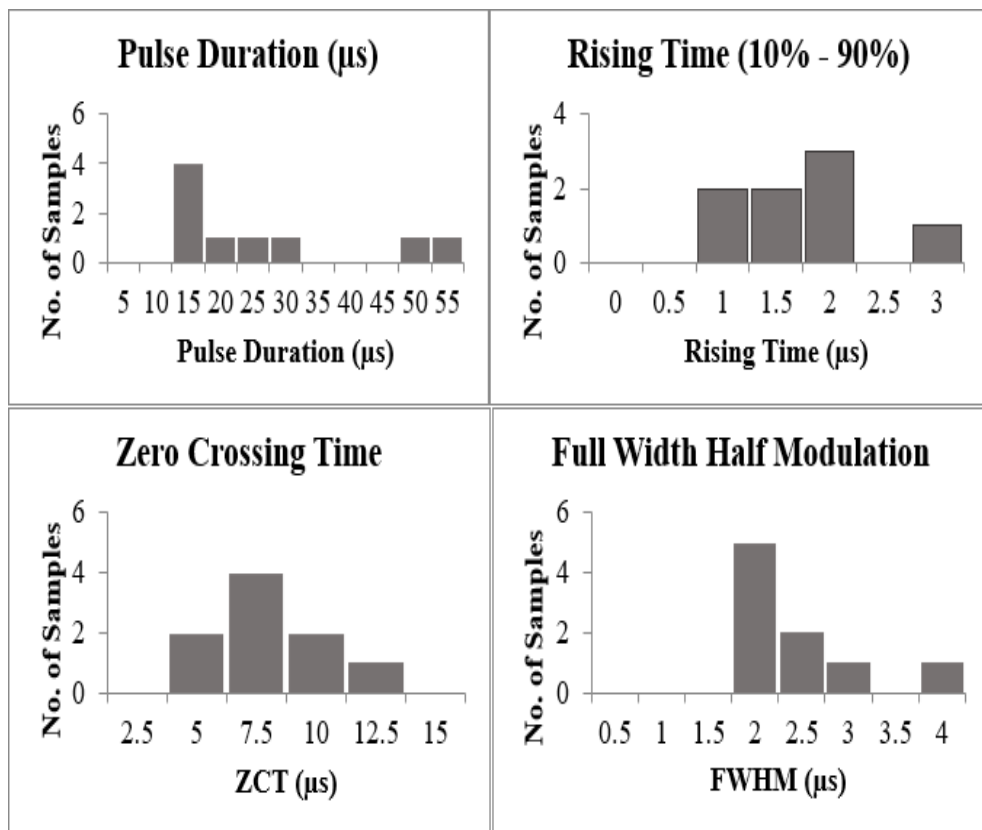


Figure 3.8: (a) Narrow Bipolar Pulse associated with negative cloud-to-ground flash and associated with the cloud flashes. (a) Pulse Duration; (b) Zero Crossing Time of NBP; (c) Time Rise (10-90%) of NBP; (d) Full Wave Half Maximum (FWHM) of NBP

Table 3.6 summarizes 9 out of the total 312 samples characterized as NBPs associated with negative ground

flashes. Of these 9 samples, 3 appeared before the Preliminary Breakdown Pulse (PBP), while 6 appeared after the first return stroke. In this analysis, we found that the number of Negative Narrow Bipolar Pulses (NNBPs) was very low and insignificant to separate from Narrow Positive Bipolar Pulses (NPBPs). Therefore, we included both polarities of NBPs as a single group. The duration of NBPs ranged from 12.80  $\mu$ s to 50.64  $\mu$ s, with arithmetic and geometric means of  $24.40 \pm 14.90$   $\mu$ s and 21.20  $\mu$ s, respectively. The ZCT ranged from 4.34  $\mu$ s to 11.91  $\mu$ s, with arithmetic and geometric means of  $7.27 \pm 2.53$   $\mu$ s and 6.89  $\mu$ s, respectively. The rise time (10–90%) ranged from 0.56  $\mu$ s to 2.59  $\mu$ s, with arithmetic and geometric means of  $1.34 \pm 0.68$   $\mu$ s and 1.19  $\mu$ s, respectively. The FWHM ranged from 1.61  $\mu$ s to 3.73  $\mu$ s, with arithmetic and geometric means of  $2.16 \pm 0.66$   $\mu$ s and 2.09  $\mu$ s, respectively. The minimum and maximum ratios (Pa/Os) were -0.69 and -0.13, respectively, with an arithmetic mean of  $-0.35 \pm 0.16$ .

Figure 3.8(a) shows the histogram for the duration of NBPs associated with negative cloud-to-ground flashes. The majority of duration pulses lie between 10 to 15  $\mu$ s, with the standard deviation being about 61.07% of the arithmetic mean. According to the histogram in Figure 3.8(b), the maximum frequency of isolated NBPs for zero crossing time (ZCT) is between 5  $\mu$ s to 7.5  $\mu$ s. The rise time (10–90%) lies between 1.5 to 2  $\mu$ s, as shown in Figure 3.8(c). The highest frequency duration of FWHM for isolated NBPs appeared between 1.5 to 2  $\mu$ s. The results of NBPs associated with cloud-to-ground flashes are shown in Table 3.6.

Next, the results in Table 3.6, were separated as NBP associated with the negative cloud-to-ground flash appear before the preliminary breakdown pulse (as depicted Table 3.7) and NBP associated with the negative cloud-to-ground flash appear after the first return (as depicted in Table 3.8). Further, by considering the arithmetic mean and geometric mean value for all parameters, we found that the parameters value between the Table 3.6 and Table 3.7 mostly are showing small difference with each other's. In details, it is found that the difference of NBP duration referring to the arithmetic mean and geometric mean are under the factor of 1.32 and 1.38 respectively.

**Table 3.6: NBP associated with the negative cloud-to-ground flash**

Features	NBP Duration ( $\mu$ s)	ZCT ( $\mu$ s)	Time Rise ( $\mu$ s) 0-100%	Rising Time ( $\mu$ s) 10%-90%	FWHM ( $\mu$ s)	Ratio Pa/Os
no of sample	9	9	9	9	9	9
min	12.80	4.34	1.67	0.56	1.61	-0.69
max	50.64	11.91	9.60	2.59	3.73	-0.13
Arith. mean	24.40	7.27	3.92	1.34	2.16	-0.35
Geo. mean	21.20	6.89	3.38	1.19	2.09	-
median	17.76	7.13	3.68	1.44	2.00	-0.35
Std. dev	14.90	2.53	2.45	0.68	0.66	0.16

Moreover, as regarding to the value of arithmetic mean and geometric mean for zero crossing are under the factor of 1.16 and 1.15 respectively. The rising time (0%-100%) and rising time (10%-90%) showed the difference of reading under the factor of 1.58 (arithmetic mean) and 1.45 (geometric mean) respectively for rising time (0% - 100%) while the factor of 1.47 (arithmetic mean) and 1.71 (geometric mean). Besides, for FWHM, they are having a difference by showing the factor value of 1.12 (arithmetic mean) and 1.08 (geometric mean). Overall, all the parameters compared between Table 3.6 and Table 3.7 shows the difference under the factor range of 1.08 to 1.71 which is proven not a big discrepancy.

**Table 3.7: NBP associated with the negative cloud-to-ground flash appear before the preliminary breakdown pulse**

Features	NBP Duration ( $\mu$ s)	ZCT ( $\mu$ s)	Time Rise ( $\mu$ s)0-100%	Rising Time ( $\mu$ s) 10%-90%	FWHM ( $\mu$ s)	Ratio Pa/Os
No. of sample	3	3	3	3	3	3
Min	17.76	4.54	1.80	0.64	1.76	-8.07
max	50.64	9.20	3.68	1.44	2.09	7.04
Arith. mean	32.16	6.29	2.47	0.91	1.95	1.60
Geo. mean	29.34	5.98	2.33	0.84	1.94	-
Median	28.08	5.12	1.92	0.65	2.00	5.85
Std. dev	16.82	2.54	1.05	0.46	0.17	8.40

By comparing between (concerning of the parameter of NBP duration, ZCT and FWHM) the results of Table 3.7 and 3.8 with the Table 3.5 and 3.6, there have shown similar results to each other. Nevertheless, the Rising Time (0% - 100%) in Table 3.6 and Table 3.8 are different compared to the result in Table 3.5 under a factor of 2.23 and 2.64, referring to their arithmetic mean respectively. Further, the time rising (10% - 90%) in Table 3.8 is different compared to the result in Table 3.5 for the arithmetic mean and geometric mean under a factor of 2.29 and 2.13. In addition, we also found that there are different of the Ratio Pa/Os between Table 3.7 and 3.5 with the factor of 5.71 for the arithmetic value. We also found significant difference of arithmetic value of Ratio Pa/Os in Table 3.8 and Table 3.5 by the factor of 47.71.

**Table 3.8: NBP associated with the negative cloud-to-ground flash appear after the first return stroke**

Features	NBP Duration ( $\mu$ s)	ZCT ( $\mu$ s)	Time Rise ( $\mu$ s)0-100%	Rising Time ( $\mu$ s) 10%-90%	FWHM ( $\mu$ s)	Ratio Pa/Os
no of sample	6	6	6	6	6	6
min	12.80	4.34	1.67	0.56	1.61	-37.96
max	47.94	11.91	9.60	2.59	3.73	4.34
Arith. mean	20.52	7.76	4.65	1.56	2.27	-13.36
Geo. mean	18.02	7.39	4.06	1.41	2.16	-
median	14.14	7.14	4.30	1.61	2.01	10.42
Std. dev	13.71	2.61	2.70	0.69	0.81	14.90

Therefore, based on this analysis work, the benefits that are gained by separating the data of Isolated NBP and NBP associated with the ground flashes can be clearly proven since the parameters of the ratio of Pa/Os have given a big discrepancy. One who are planning to analyse a sub-microsecond structure of the pulse must separate between the isolated case and with the NBP associated with flashes (ground flashes or cloud flashes).

#### 4. CONCLUSION

The Narrow Bipolar Pulses (NBPs) from the South-West Monsoon season (May 2018) and the North-East Monsoon (November 2016) were successfully analyzed, as detailed in Section 3. From a total of 149 samples collected during the South-West Monsoon, 22 were identified as isolated NBPs, while 127 were associated with cloud-to-ground (CG) and cloud flashes.

In contrast, during the North-East Monsoon, 55 NBP samples were gathered, of which 46 were classified as isolated NBPs. These included 9 positive and 37 negative polarity NBPs. Additionally, 9 samples were

characterized as NBPs associated with negative CG flashes. Among these 9 samples, 3 occurred before the Preliminary Breakdown Pulse (PBP), while 6 occurred after the first return stroke.

The evaluation of data during the South-West Monsoon, focusing on lightning parameters, reveals similarities in parameter values among isolated Narrow Bipolar Pulses (NBPs), mixed NBPs associated with negative cloud-to-ground (CG) flashes, and NBPs associated with cloud flashes. However, when NBPs linked to negative CG flashes and those associated with cloud flashes are separated and compared with isolated NBPs, distinct differences emerge in parameters such as Full Width at Half Maximum (FWHM), amplitude ratio, and overshoot. These differences are evident both in NBPs preceding the Preliminary Breakdown Pulse (PBP) of negative CG flashes and in NBPs appearing after the first return stroke.

Comparative analysis during the North-East Monsoon highlights variations in lightning parameters, particularly NBP duration, Zero-Crossing Time (ZCT), and FWHM. Key findings include:

- i) The Rising Time (0%–100%) for NBPs associated with ground flashes and NBPs occurring after ground flashes shows minor differences compared to isolated NBPs, with arithmetic mean factors of 2.23 and 2.64, respectively. Furthermore, the Rising Time (10%–90%) for NBPs occurring after ground flashes differs from isolated NBPs by factors of 2.29 and 2.13 for the arithmetic and geometric means, respectively.
- ii) The Ratio of Peak Amplitude to Overshoot (Pa/Os) differs significantly between NBPs preceding ground flashes and isolated NBPs, with a factor of 5.71 for the arithmetic mean. A notable difference is also observed for NBPs occurring after ground flashes compared to isolated NBPs, with an arithmetic mean factor of 47.71.

Our findings suggest that separating these cases is essential for accurate statistical analysis of NBPs. The most significant conclusion from this study is that the total occurrence of NBPs during the North-East Monsoon is substantially lower than during the South-West Monsoon. This indicates that tropical monsoon seasons influence the production of Narrow Bipolar Pulses

#### ACKNOWLEDGMENT

The authors sincerely thank the Faculty of Electrical Engineering Technology (FTKE) and the Centre for Research and Innovation Management (CRIM) at Universiti Teknikal Malaysia Melaka (UTeM) for their invaluable support and the provision of measurement facilities during the campaign conducted from 2015 to 2019. Our gratitude also extends to the Ministry of Higher Education (MOHE) for their funding, which enabled access to essential equipment. The high-definition transient recorder, acquired through MOHE grants ERGS/2013/FKE/TK02/UTEM/03/01 and FRGS/2/2014/TK03/FTK/03/F00248, was instrumental in this study.

#### REFERENCES

- [1] T. A. L. N. Gunasekara, M. A. Z. K. W. Gunathilaka, and W. C. K. Wijewickrama, "Electric field signatures of narrow negative bipolar pulse activities from lightning observed in Sri Lanka," in *Proc. 2014 Int. Conf. Lightning Protection (ICLP)*, Shanghai, China, Oct. 2014, pp. 624–628. DOI: 10.1109/ICLP.2014.7004241.
- [2] M. Ahmad, Z. Zakaria, M. F. Mohamed, and N. Zakaria, "Latitude dependence of narrow bipolar pulse emissions," *Journal of Atmospheric and Solar-Terrestrial Physics*, vol. 128, pp. 40–45, 2015. DOI: 10.1016/j.jastp.2015.02.012.
- [3] S. Karunarathne, T. Marshall, M. Stolzenburg, and N. Karunarathna, "Observations of positive narrow bipolar pulses," *Journal of Geophysical Research: Atmospheres*, vol. 120, no. 12, pp. 7128–7143, 2015. DOI: 10.1002/2015JD023920.
- [4] T. Wu, S. Yoshida, and T. Ushio, "Observations of narrow bipolar events initiating regular lightning flashes," in *Proc. 2014 URSI Gen. Assembly and Sci. Symp. (URSI GASS)*, Beijing, China, Aug. 2014, pp. 1–4. DOI: 10.1109/URSIGASS.2014.6929517.
- [5] Z. Zakaria, M. F. Mohamed, and M. Ismail, "Wavelet analysis of narrow bipolar pulses in tropical region," in *Proc. 2017 Int. Conf. Electrical Eng. Computer Science (ICECOS)*, Penang, Malaysia, Nov. 2017, pp. 280–284. DOI: 10.1109/ICECOS.2017.8276402.
- [6] T. A. L. N. Gunasekara, W. C. K. Wijewickrama, and N. Karunarathna, "Characteristics of narrow bipolar pulses observed from lightning in Sri Lanka," *Journal of Atmospheric and Solar-Terrestrial Physics*, vol. 138, pp. 66–73, 2016. DOI: 10.1016/j.jastp.2015.12.001.

- [7] S. Karunarathne, T. Marshall, M. Stolzenburg, and N. Karunarathne, "Electrostatic field changes and durations of narrow bipolar events," *Journal of Geophysical Research: Atmospheres*, vol. 121, no. 17, pp. 10,161–10,174, 2016. DOI: 10.1002/2016JD025199.
- [8] M. R. Ahmad, S. A. S. Baharin, M. H. M. Sabri, and V. Cooray, "Very high frequency radiation emitted by negative narrow bipolar events occurred over Malacca Strait," *Journal of Atmospheric and Solar-Terrestrial Physics*, vol. 259, pp. 1–7, 2024, doi: 10.1016/j.jastp.2024.106252.
- [9] S. S. Watson and T. Marshall, "Current propagation model for a narrow bipolar pulse," *Geophysical Research Letters*, vol. 34, no. 19, 2007. DOI: 10.1029/2007GL031188.
- [10] F. Liu, X. Shao, and X. Z. Zhang, "A simple current waveform model for narrow bipolar pulses," in *Proc. 2018 Int. Conf. Lightning Protection (ICLP)*, Guangzhou, China, Oct. 2018, pp. 1–6. DOI: 10.1109/ICLP.2018.8588196.
- [11] T. Hamlin, T. E. Light, X. Shao, K. Eack, and J. Harlin, "Estimating lightning channel characteristics of positive narrow bipolar events using intrachannel current reflection signatures," *Journal of Geophysical Research*, vol. 112, no. D10, 2007. DOI: 10.1029/2006JD007370.
- [12] S. R. Sharma, M. Fernando, and V. Cooray, "Narrow positive bipolar radiation from lightning observed in Sri Lanka," *Journal of Atmospheric and Solar-Terrestrial Physics*, vol. 70, no. 9, pp. 1251–1260, 2008. DOI: 10.1016/j.jastp.2007.11.011.
- [13] N.A. Ahmad, M. Fernando, Z.A. Baharudin, V. Cooray, H. Ahmad, and Z. Abdul Malek, 2010: "Characteristics of narrow bipolar pulses observed in Malaysia," *Journal of Atmospheric and Solar-Terrestrial Physics*, Vol 72, pp. 534-540, 2010.
- [14] N. A. Ahmad, M. Fernando, and V. Cooray, "On the derivatives of narrow bipolar pulses," in *Proc. 2010 Int. Conf. Lightning Protection (ICLP)*, Nanjing, China, Sep. 2010, pp. 1–4. DOI: 10.1109/ICLP.2010.5622769.
- [15] T. Wu, W. Dong, Y. Zhang, and T. Wang, "Comparison of positive and negative intracloud discharges," *Journal of Geophysical Research*, vol. 116, no. D03111, pp. 1–9, 2011. DOI: 10.1029/2010JD015197.
- [16] V. Cooray, J. D. Borrero, and T. Y. Lee, "Electromagnetic fields of a relativistic electron avalanche with special attention to the origin of lightning signatures known as narrow bipolar pulses," *Atmospheric Research*, vol. 149, pp. 346–358, 2014. DOI: 10.1016/j.atmosres.2014.06.001.
- [17] M. R. M. Esa, M. Ahmad, and V. Cooray, "Wavelet profile of initial breakdown process accompanied by narrow bipolar pulses," *Journal of Atmospheric and Solar-Terrestrial Physics*, vol. 129, pp. 37–44, 2014. DOI: 10.1016/j.jastp.2014.07.010.
- [18] N. A. Isa, Z. A. Baharudin, I. N. A. Daud, and H. Zainuddin, "Combination of narrow bipolar pulses and attempted leaders in Melaka, Malaysia," *Indonesian Journal of Electrical Engineering and Computer Science*, vol. 25, no. 3, pp. 1825–1830, 2022. DOI: 10.11591/ijeecs.v25.i3.1825-1830.
- [19] C. Gomes and V. Cooray, "Radiation field pulses associated with the initiation of positive cloud-to-ground lightning flashes," *Journal of Atmospheric and Solar-Terrestrial Physics*, vol. 66, no. 9, pp. 1047–1055, 2004. DOI: 10.1016/j.jastp.2004.01.015.
- [20] C. Schultz, "Negative narrow bipolar lightning needs critical cloud height," *Eos, Transactions American Geophysical Union*, vol. 94, no. 14, pp. 148, 2013. DOI: 10.1002/2013EO140004.
- [21] Z. A. Baharudin, N. A. Ahmad, J. S. Mäkelä, M. Fernando, and V. Cooray, "Negative cloud-to-ground lightning flashes in Malaysia," *Journal of Atmospheric and Solar-Terrestrial Physics*, vol. 108, pp. 61–67, 2014. DOI: 10.1016/j.jastp.2013.12.001.
- [22] Z. A. Baharudin, "Characterizations of Ground Flashes from Tropic to Northern Region," Doctoral thesis, comprehensive summary, Acta Universitatis Upsaliensis, 2014.
- [23] Z. A. Baharudin, V. Cooray, M. Rahman, P. Hettiarachchi, N. A. Ahmad, "On the characteristics of positive lightning ground flashes in Sweden," *Journal of Atmospheric and Solar-Terrestrial Physics*, vol. 138, pp. 106–111, 2016. DOI: 10.1016/j.jastp.2015.11.006.
- [24] P. N. S. A. Rahman, Z. Baharudin, N. H. A. Rahim, "Misidentification of type of lightning flashes in Malaysia," *TELKOMNIKA Indonesian Journal of Electrical Engineering*, vol. 12, no. 8, pp. 5938–5945, 2014. DOI: 10.11591/telkomnika.v12i8.4341.
- [25] A. R. Ramlee, N. A. Ahmad, Z. A. Baharudin, and Mohamed, "High-speed video observations on fork lightning events in Malaysia," *Indonesian Journal of Electrical Engineering and Computer Science*, vol. 19, no. 3, pp. 1620–1625, 2020. DOI: 10.11591/ijeecs.v19.i3.1620-1625.
- [26] A. F. Munauwer, Z. A. Baharudin, M. A. M. Hanafiah, M. Zainon, S. N. S. Salim, and M. Ibrahim, "Unravel the extent of the existence of positive ground flash in Malaysia," *International Journal of Emerging Trends in Engineering Research*, vol. 8, no. 1.1, pp. 166–169, 2020. DOI: 10.30534/ijeter/2020/02812020.
- [27] N. A. Isa, Z. A. Baharudin, A. R. M. Ismail, Z. Zakaria, A. I. A. Rahman, and A. A. Zulkefle, "On the existence of attempted leader in tropical thunderstorm," *International Journal of Emerging Trends in Engineering Research*, vol. 8, no. 1.1, pp. 153–157, 2020. DOI: 10.30534/ijeter/2020/01812020.